Fire response of ultra high performance concrete beams

Banerji S.[a], Kodur V.K.R.[b] and Solhmirzaei R.[a]

[a]PhD student, Department of Civil and Environmental Engineering, Michigan State University, East Lansing, MI, USA.
[b]University Distinguished Professor, Department of Civil and Environmental Engineering, Michigan State University, East Lansing, MI, USA.

Abstract:

This paper presents a macroscopic finite element model for assessing the fire performance of UHPC beams. In the model, fire resistance analysis is carried out at incremental time steps under the combined effects of fire exposure and structural loading till failure of the beam. The model accounts for high temperature properties of constituent materials and incorporates the progression of fire induced spalling utilizing a hygro-thermo-mechanical spalling sub-model. The developed model is validated by comparing predicted response parameters with measured data from fire tests on UHPC beams. Results from the analysis indicate that UHPC beams can have lower fire resistance, as compared to conventional normal strength concrete beams. The progression of spalling inside the beam section and its effect on failure time is discussed.

Keywords: Ultra high performance concrete; Fire induced spalling; Numerical model; Pore pressure; Fire resistance; UHPC beams

1. Introduction

In recent years, the use of Ultra High Performance Concrete (UHPC) in infrastructure projects has increased owing to its high compressive and tensile strength and improved durability properties (Graybeal and Tanesi 2007; Gu et al. 2015). Often, steel fibers are added to UHPC to increase ductility and durability characteristics of concrete (Gangwar et al. 2018). High durability in UHPC is attributed to its low permeability through dense and compact microstructure created by high fineness admixtures. However, previous research studies (Kodur and Dwaikat 2008, Lee et al. 2012, Kahanji et al. 2016) have shown that high strength concretes, unlike conventional Normal Strength Concrete (NSC), may not exhibit good fire performance and are susceptible to fire induced spalling.

The break-up of concrete chunks from structural member during fire exposure is termed as fire induced spalling. Such spalling has the effect of reducing the cross sectional area of the structural member and increasing heat penetration to the steel reinforcement. Thus, spalling might lead to reduction in strength and stiffness of reinforced concrete (RC) members, which in turn might cause early failure of RC members under certain fire conditions (Kodur 2000).

Currently, there are limited experimental studies on the fire response of UHPC members. Much of the reported data on fire performance of UHPC is at material level, involving small scale tests on cubes, cylinders and prisms. Very few studies on full scale UHPC members are carried out by researchers (Pimienta et al. 2011, Kahanji et al. 2016). Although, there are several numerical studies on fire resistance evaluation for RC beams, studies accounting for spalling are very limited (Dwaikat and Kodur 2009, Gawin et al. 2006, Zhang and Davie 2013). Prediction of

fire resistance of high strength beams is not realistic without taking effects of spalling into account. Further, majority of the reported numerical models for spalling are for High Strength Concrete (HSC) members. At present, there is no analytical model to trace the fire response of UHPC beams.

To overcome some of the current knowledge gaps, a macroscopic finite element numerical model using FORTRAN program is developed for tracing performance of UHPC beams under fire exposure conditions. A simplified hygro-thermo-mechanical spalling sub-model is incorporated to account for fire induced spalling. This paper presents the details of the numerical model to determine the temperature distribution, the extent of spalling and fire resistance of UHPC beams. The numerical model is validated against results and observations obtained from full scale fire resistance tests on UHPC beams.

2. Numerical Model

A macroscopic finite element based numerical model was originally developed by Kodur and Dwaikat (2008), for evaluating fire performance of RC beams. Spalling in this model was accounted by using pore pressure mechanism (Dwaikat and Kodur 2009). This model is extended to trace the response of UHPC beams under combined effects of fire exposure and structural loading. The updated model accounts for temperature induced degradation of UHPC, tensile post-cracking behavior of UHPC, and spalling by pore pressure and thermo-mechanical mechanism.

2.1. Analysis Procedure

In the fire resistance analysis, the given beam is idealized by dividing it into a number of segments along its length and the mid-section of each segment is assumed to represent the overall behavior of the segment. This cross-section representing each segment is further discretized into a number of elements. At each time step, fire resistance analysis is carried out in three stages namely, (1) establishing fire temperatures resulting from fire exposure; (2) carrying out heat transfer analysis to calculate temperature distribution and evaluating pore pressure within the concrete cross-section; (3) performing strength analysis of the member (beam). In stage 3, temperature dependent moment-curvature relations are generated for various beam segments. The output response parameters generated at each time step, from the developed program, include temperatures at various locations, stress due to mechanical loading, thermal stress and pore pressure. A flow chart illustrating various steps in tracing the fire response of beams is shown in Figure 1.

Using the generated stress values, the stress at a given time step is evaluated as the resultant of three stresses namely pore pressure, thermal and mechanical stresses. Then the resultant stress acting on each concrete element is compared against the temperature dependent concrete strength to determine if the element has spalled at that time step. At each time step, response parameters from the thermal and structural analysis are utilized to evaluate the state of the beam under different failure limit states. The analysis at a specified time step terminates if failure is attained; otherwise, the analysis continues to next time step.

2.2. High Temperature Material Properties

To simulate the fire response of UHPC beam, temperature dependent thermal and mechanical properties of concrete and reinforcing steel are to be supplied as input data to the model. For

UHPC, design codes do not provide any specific relations for high temperature thermal and mechanical properties. Hence, thermal property relations are incorporated from experimental studies conducted by researchers on material characterization of steel fiber reinforced reactive powder concrete (RPC), whose behavior is representative to that of UHPC (Abid et al. 2017).
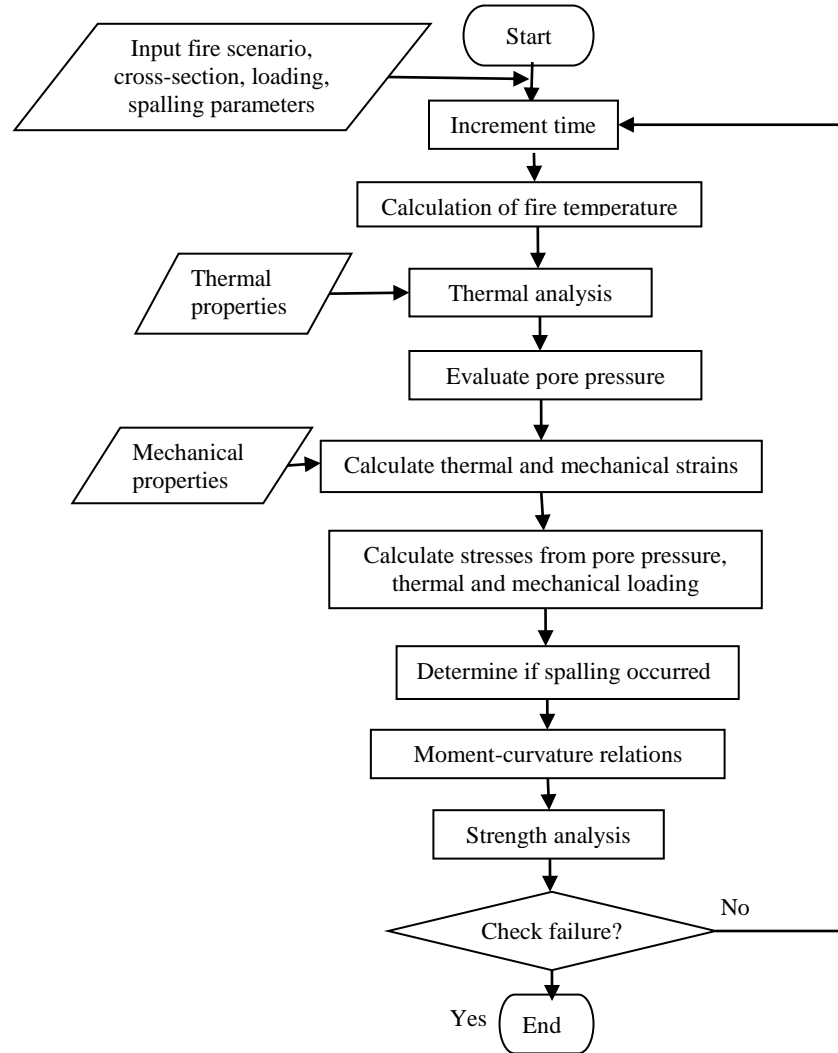
Figure 1. Flow chart illustrating steps in the numerical model for fire resistance analysis of concrete beams

Relations for thermal conductivity and specific heat variation with temperature for steel reinforced RPC are utilized for this study as specified by Zheng et al. (2014). For high temperature mechanical properties of UHPC, compressive and tensile stress-strain relationships for steel fiber reinforced RPC are incorporated from the studies conducted by Zheng et al. (2015). as shown in Figure 2. The temperature induced tensile and compressive strength degradation is adopted from Zheng et al. (2013). For reinforcing steel, the mechanical properties (stress–strain–temperature relationships) that are given in the Eurocode 2 are incorporated into the model.

2.3. Spalling Evaluation

Fire-induced spalling in concrete can be explained based on two mechanisms, namely pore pressure buildup and brittle fracture (Bazant 1997). In the pore pressure buildup mechanism,

vaporization of moisture takes place in heated concrete. Due to low permeability in high strength concretes, the vapor is unable to escape and leads to high pressure buildup, which exerts tensile stress on the concrete member. According to the brittle fracture mechanism, thermal stresses at high temperatures get developed inside the heated surface in a concrete member. These thermal stresses lead to storing of high potential energy in the concrete member and sudden release of this energy results in brittle fracture and spalling of concrete.
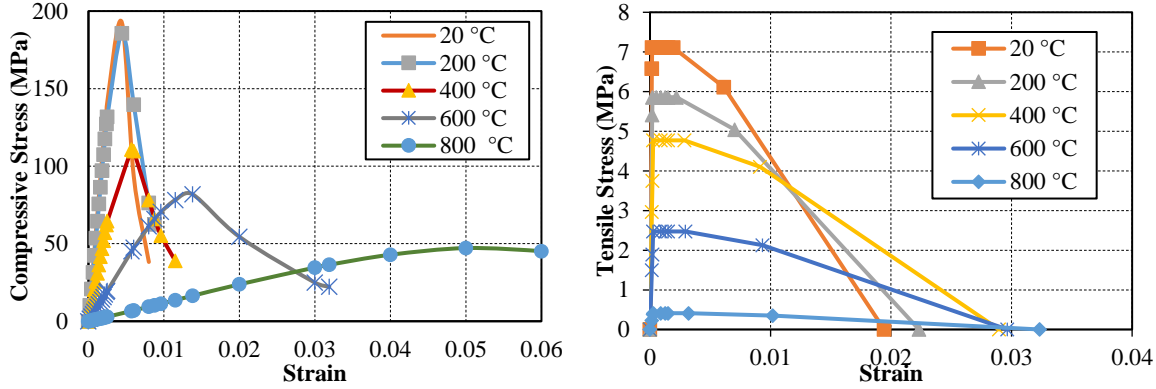

Figure 2. Stress-strain response of UHPC at different temperatures

To incorporate both the spalling mechanisms, stresses due to temperature induced vapor pressure, thermal strains and mechanical loading on the beam are to be considered. The first component of stress, is due to the pore pressure in concrete which can be evaluated through a hydrothermal model (Dwaikat and Kodur 2009). This hydrothermal model uses the principles of mechanics and thermodynamics, to predict pore pressure in a concrete member exposed to fire. The mass transfer equation for water vapor generated inside heated concrete can be written as:

$$A\left(\frac{dP_v}{dt}\right) = \nabla B \nabla P_v + C \tag{1}$$

where, P_v is the pore pressure, t the time, A, B and C are the parameters that depend on temperature, rate of increase in temperature, permeability of concrete, initial moisture content, and the isotherms used in analysis. The permeability value of UHPC is selected as 2.2 x 10^{-18} m^2 according to gas permeability tests conducted by Li et al. (2018). Finite element analysis is used to solve Eq. 1 and to compute pore pressure (P_v) distribution. The tensile stress exerted due to pore pressure (σ_p) is determined by multiplying pore pressure (P_v) with Biot's coefficient, which is considered as 0.8 from the previous studies of Ichikawa and England (2004).

The second component of the stress is the fire induced thermal stress (σ_{th}) which can be evaluated knowing the temperatures in the beam cross-section. The thermal stress is evaluated by utilizing the high temperature material properties and thermal expansion of concrete. The third stress component, load induced (mechanical) stress (σ_l) can be evaluated by mechanical strain component and high temperature mechanical properties (stress-strain relationships) at any given time step. Mechanical stress significantly increases with increasing temperature due to degradation of strength properties of concrete and steel. Further, fire induced spalling leads to reduction of beam cross-section and higher mechanical stresses in the beam.

In each concrete element, the resultant stresses (tensile or compressive) are checked against temperature dependent concrete strength (tensile, f'$_{tT}$ or compressive, f'$_{cT}$) to determine spalling at each time step of the analysis as illustrated in Figure 1. Tensile stress is the sum of stresses due to pore pressure, thermal and mechanical loading, whereas resultant compressive stress comprises of stresses due to thermal and mechanical loading. If the stress exceeds the strength, that element is considered as spalled and is removed from subsequent analysis steps.

Spalling is evaluated only in uncracked elements (strain is lower than tensile cracking strain), as cracks create escape channels for release of pore pressure lowering the spalling propensity. The geometry and boundary conditions are updated for subsequent analysis steps.

2.4. Failure Limit States

At each time step, the failure of the UHPC beams is checked based on strength and deflection failure criteria as specified in ASTM E119. Accordingly, failure is said to occur when the moment carrying capacity of the beam exceeds the subjected moment due to the applied load. In addition, deflection limit state can also play a major role on response of beams exposed to fire conditions due to faster degradation of member stiffness at elevated temperature. According to ASTM E119, failure of beam is said to occur when mid-span deflection exceeds $L^2/400d$ or the rate of deflection exceeds $L^2/9000d$ (mm/min) where, L is the span length of the beam (mm) and, d is the effective depth of the beam (mm).

3. Model Validation

The numerical model is validated against measured data from fire tests on UHPC beams. Experimentally measured mid-span deflection, temperatures at various locations and extent of spalling are compared with model predictions.

3.1. Selection of Beams

Fire resistance test on two UHPC beams, designated as U-B1 and U-B2 was undertaken at Michigan State University for validating the model. Both beams are of rectangular cross section, 180 mm in width, 270 mm in depth, and had a length of 4000 mm. To take full advantage of the high compressive and tensile strength offered by UHPC, no compression and shear reinforcement (stirrups) were provided in these beams. The beams were reinforced with three rebars of 13 mm diameter and yield strength of 435 MPa as tensile reinforcement. The cross-sectional details and instrumentation configuration for the test beams are shown in Figure 3. Both beams were instrumented with thermocouples, strain gauges and displacement transducers.
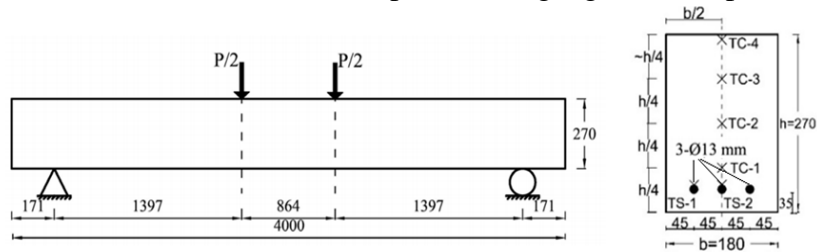

Figure 3. Cross section of tested UHPC beams (All dimensions are in mm)

3.2. Analysis Details

Fire resistance tests on the UHPC beams U-B1 and U-B2 were carried out using a structural fire testing furnace located in the Civil Infrastructure Lab at Michigan State University. Each beam was placed into the furnace, and subjected to three-side fire exposure with a combination of structural loading as shown in Figure 3. Test and analysis parameters are tabulated in Table 1. The mesh dimensions of the macroscopic FEM are considered as 10x10 mm.

Both the UHPC beams were tested under ASTM E-119 standard fire exposure, but were subjected to different load levels in terms of load ratio. Load ratio is the ratio of applied load on

the beam under fire conditions to the load carrying capacity of the beam at room temperature. Beams U-B1 and U-B2 were subjected to 40% and 60% load ratio respectively. The loading was applied 30 minutes prior the start of the fire and this loading was stabilized till no further increase in beam deformation could be measured. The applied load was then maintained constant throughout the duration of fire exposure. After each beam cooled down fully to ambient temperature, detailed observations on extent of spalling was measured.

Table 1. Summary of test parameters for UHPC beams used in the analysis

Test beam	Aggregate type	Room temperature capacity (kNm)	Test day compressive strength f'$_c$ (MPa)	Test day tensile strength f'$_t$ (MPa)	Permeability (m^2)	Applied loading (% of capacity)	Fire exposure
U-B1	Carbonate	67.8	193	7	2.2 x 10^{-18}	40	ASTM E-119
U-B2	Carbonate	67.8	193	7	2.2 x 10^{-18}	60	ASTM E-119

3.3. Comparison of Thermal Response

The measured and predicted temperatures at rebar and cross-sectional locations in beams U-B1 and U-B2 are plotted in Figure 4. The temperatures in beam U-B1 are somewhat overestimated after 20 minutes of fire exposure. This might be due to the incorporation of thermal properties of RPC instead of UHPC owing to lack of specific high temperature thermal properties for UHPC.
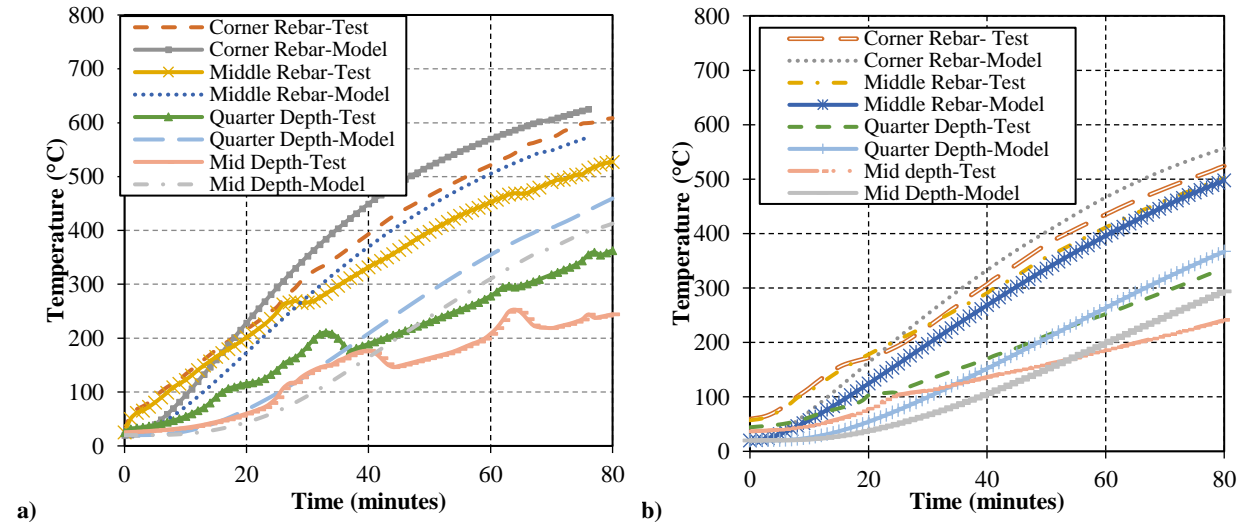
Figure 4. Predicted and measured temperature progression in UHPC beams: a) U-B1, b) U-B2

Further, beam U-B1 experienced higher amount of severe spalling during fire test than U-B2, due to which moisture evaporation was significant in the beam. Thermal energy was utilized for this process of moisture evaporation, which lowered the temperatures, as can be seen in the plateaus of time-temperature response curve plotted in Figure 4. In general, there is reasonable agreement between the measured and predicted temperatures for beam U-B2. Although beam U-B2 also had severe spalling but, it was about 50% less than beam U-B1 due to higher level of microcracks developing in the beam, resulting from higher applied load on beam U-B2.

3.4. Comparison of Structural Response

The predicted and measured mid-span deflection in UHPC beams U-B1 and U-B2 are shown in Figure 5(a). Overall, the predicted deflection in both beams follows that of measured ones. The

deflection response can be grouped into three stages. In stage 1, in the first 40 minutes of fire exposure, deflections in both the beams increase at a slow steady rate. This deflection can be attributed to the thermal strains generated due to high thermal gradients that develop along the beam depth. Spalling occurred in both the beams after 10 minutes of fire exposure, with higher level of spalling in beam U-B1, than beam U-B2. However, concrete and steel reinforcement undergo very little strength degradation in this stage due to low temperatures in beam cross-section. Thus, the effects of spalling are not significant in this stage.

In stage 2, after 40 minutes into fire exposure up to 60 minutes, deflections in both beams U-B2 increases at a rapid pace. The increase in deflection in stage 2, results mainly due to degradation of strength and stiffness in concrete and steel reinforcement, as temperatures increase in inner layers of the beam. Both the beams experienced severe spalling in this stage and this accelerated high temperature propagation. This effect of spalling is more pronounced for beam U-B1 in stage 2 leading to a faster rate of increase in deflection than U-B2.

Finally, in stage 3 beyond 60 minutes, deflections increase very rapidly and are due to significant loss of strength and stiffness, as well as high temperature creep effects. Both the beams fail after around 75 minutes of fire exposure. Despite, being subjected to lower load level, beam U-B1 fails at the same time as beam U-B2 due to high levels of spalling in this beam. The model predictions underestimate the final deflections. This may be due to the discrepancy between the actual high-temperature properties and those used in the analysis.
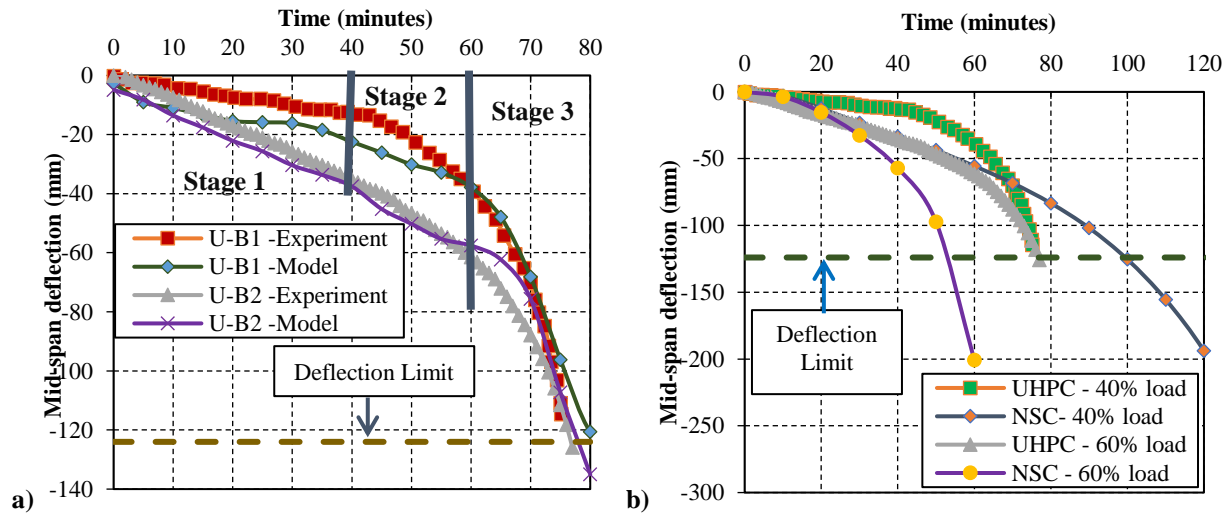

Figure 5. Comparison of measured mid-span deflections for test beams U-B1 and U-B2 with predicted deflections of a) U-B1 and U-B2 ; b) normal strength concrete beams

3.5. Comparison of Spalling and Fire Resistance

In the model, spalling volume of concrete was calculated by comparing the reduced cross section, after removing the spalled elements from the original cross-section, at the end of fire resistance analysis. Spalling during fire tests was monitored through visual observations. Visual observations indicated that spalling initiated in both the beams after 10 minutes of fire exposure and was violent in nature. Following the test, the beam was allowed to cool down and volumetric measurements of the tested beam were taken. Both the UHPC beams suffered severe spalling. However, the extent of spalling was higher in beam U-B1 than beam U-B2. This can be attributed to the variation of cracking in both the beams (see Figure 6). The high density of cracks in the tensile zone of beam U-B2 under higher loading led to the release of pore pressure build-up, resulting in less spalling. The analysis results indicate the same by considering no

spalling in the cracked elements. The predicted and measured extent of spalling is shown in Table 2 and have reasonable agreement.

The fire resistance of the UHPC beams was evaluated using the numerical model based on the strength and deflection failure limit states. The fire resistance of beam U-B1 obtained from the analysis, based on the strength failure limit state was 75 minutes, which aligns well with the measured fire resistance in the test (75 minutes). The failure of U-B1 is governed by strength limit state due to faster strength degradation caused by severe spalling. According to the model, the fire resistance of beam U-B2 was 75 minutes based on the strength failure limit state which is lower than fire resistance based on deflection limit state (78 minutes). However, the failure times lie close to each other and agree with the measure fire resistance (78 minutes). The measured and predicted fire resistance values are tabulated in Table 2.

Table 2. Summary of results from model and tests

UHPC test beam	Applied loading (% of capacity)	Final deflection (mm)		Fire resistance (minutes)			Extent of spalling (%)		Spalling level
		Test	Model	Test	Model		Test	Model	
					Strength	Deflection			
U-B1	40	118	96	75	75	82	13.3	12	Severe
U-B2	60	126	105	78	75	78	7.5	7	Severe
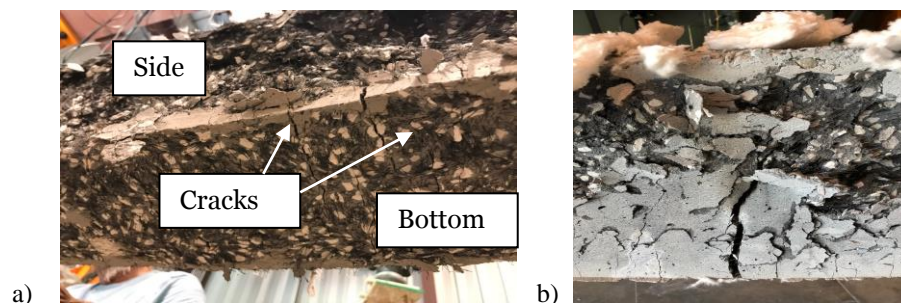
Figure 6. Tensile cracking during fire exposure in beams: a) U-B1, b) U-B2

It is evident that the level of spalling plays an important role in fire response of UHPC beams. To further assess the effect of spalling, the structural response of UHPC beams is compared with that of conventional normal strength concrete (NSC) beams of same cross-sectional configuration, test conditions and subjected to the same load levels of 40% and 60% as the tested UHPC beams, simulated utilizing the model and shown in Figure 5(b). The compressive strength of NSC beam is considered as 30 MPa and its tensile strength is neglected. The permeability of NSC beam is considered high (2×10^{-16} m^2) as recommended by (Boel et al. 2008) and this resulted in no spalling during entire fire exposure. When subjected to load level of 60% of ambient bending strength (as beam U-B2), NSC beam failed about 20 minutes earlier than UHPC beam. This early failure is due to the inability of NSC beam to withstand high load levels and can be attributed to the extremely low stiffness owing to absence of steel fibers in NSC, compared to UHPC. At 40% load level scenario (as beam U-B1), NSC beam failed at 100 minutes which is 25 minutes higher than UHPC beam. From this study, it is evident that spalling plays a major role in deteriorating the stiffness of the UHPC beam and higher extent of spalling results in significantly poor fire resistance of UHPC beam compared to NSC beam.

The failure times for both the beams are almost the same, despite lower level of load applied on U-B1 (40%) than U-B2 (60%). Due to higher loading, U-B2 developed severe cracks (as seen in tests) in comparison to U-B1, along with a macro-crack as shown in Figure 6. The

higher density of cracks in beam U-B2 helped in creating escape channels for release of developed high pore pressure in UHPC and lowered the severity of spalling. It is evident that the level of spalling plays an important role in fire response of UHPC beams. Spalling affects the rate of degradation of material strength and leads to faster penetration of heat, resulting in early failure even at lower load levels.

4. Conclusions

Based on the results and observations presented in this paper, following conclusstions can be drawn on the fire behavior of UHPC beams:
- Proposed macroscopic finite element based numerical model is capable of tracing the behavior of UHPC beams under fire conditions.
- UHPC beams are highly susceptible to spalling and can have significantly lower fire resistance than that of conventional NSC beams.
- Load level applied on the beam has an effect on the extent of spalling that occur in UHPC beams. Higher loading lead to more cracking and this facilitates release of pore pressure resulting in less extent of spalling.

5. Acknowledgements

References

Abid, M., Hou, X., Zheng, W. & Hussain, R. R., 2017. High temperature and residual properties of reactive powder- A review. *Construction and Building Materials,* 147(2017), pp. 339-351.

ASTM E119-18, 2018. *Standard Test Methods for Fire Tests of Building Construction and Materials,* West Conshohocken, PA: ASTM International.

Bazant, Z. P., 1997. *Analysis of Pore Pressure, Thermal Stress and Fracture in Rapidly Heated Concrete.* Gaithersburg,Maryland, 155-164, Int. Workshop on Fire Performance of High Strength Concrete, NIST.

Boel, V., Audenaert, K. & Schutter, G. D., 2008. Gas permeability and capillary porosity of self-compacting concrete. *Journal of Materials and Structures,* 41(7), pp. 1283-1290.

Dwaikat, M. B. & Kodur, V., 2009. Hydrothermal model for predicting fire-induced spalling in concrete. *Fire Safety Journal,* 44(2009), pp. 425-434.

Dwaikat, M. & Kodur, V., 2009. Response of restrained concrete beams under design fire exposure. *Journal of Structural Engineering,* 135(2009), pp. 1408-1417.

Eurocode2, 2004. *EN 1992-1-2 design of concrete structures, Part 1-2: general rulesstructural fire design.* Brussels, Belgium: European Committee for Standardization.

Gangwar, S., Mishra, S. & Sharma, H. K., 2018. *An Experimental Study on Mechanical Properties of Ultra-High-Performance Fiber-Reinforced Concrete (UHPFRC).* Singapore, Lecture Notes in Civil Engineering, vol 25. Springer.

Gawin, D., Pesavento, F. & Schrefler, B. A., 2006. Towards prediction of the thermal spalling risk through a multi-phase porous media model of concrete. *Computer Methods in Applied Mechanics and Engineering,* 195(41-43), pp. 5707-5729.

Graybeal, B. & Tanesi, J., 2007. Durability of an Ultrahigh-Performance Concrete. *Journal of Materials in Civil Engineering,* 19(10), pp. 848-854.

Gu, C. P., Ye, G. & Sun, W., 2015. Ultrahigh performance concrete-properties, applications and perspectives. *Science China Technological Sciences,* 58(4), p. 587–599.

Ichikawa, Y. & England, G. L., 2004. Prediction of moisture migration and pore pressure buildup in concrete at high temperatures. *Nuclear Engineering and Design,* Volume 228, pp. 245-259.

Kahanji, C., Ali, F. & Nadjai, A., 2016. Explosive spalling of ultra-high performance fibre reinforced concrete beams under fire. *Journal of Structural Fire Engineering,* 7(4), pp. 328-348.

Kodur, V., 2000. *Spalling in high strength concrete exposed to fire––concerns, causes, critical parameters and cures.* Philadelphia, USA, ASCE, pp 1-8.

Kodur, V. & Dwaikat, M. B., 2008. Effect of Fire Induced Spalling on the Response of Reinforced Concrete Beams. *International Journal of Concrete Structures and Materials,* 2(2), pp. 71-81.

Kodur, V. et al., 2018. Analysis of flexural and shear resistance of ultra high performance fiberreinforced concrete beams without stirrups. *Engineering Structures,* 174(2018), pp. 873-884.

Lee, J. H., Sohn, Y. S. & Lee, S. H., 2012. Fire resistance of hybrid fibre-reinforced,ultra-high-strength concrete columns with compressive strength from 120 to 200 MPa. *Magazine of Concrete Research,* 64(6), pp. 539-550.

Li, Y., Tan, K. H. & Yang, E. H., 2018. Influence of aggregate size and inclusion of polypropylene and steel fibers on the hot permeability of ultra-high performance concrete (UHPC) at elevated temperature. *Construction and Building Materials,* Volume 169, pp. 629-637.

Pimienta, P., Mindeguia, J., Simon, A. & Behloul, M., 2011. Behaviour of UHPFRC at high temperatures. In: F. a. R. J. Toutlemonde, ed. *Designing and Building with UHPFRC.* Hoboken, NJ: John Wiley & Sons, pp. 579-600.

Zhang, H. L. & Davie, C. T., 2013. A numerical investigation of the influence of pore pressures and thermally induced stresses for spalling of concrete exposed to elevated temperatures. *Fire Safety Journal,* Volume 59, pp. 102-110.

Zheng, W., Li, H. & Wang, Y., 2013. Compressive and tensile properties of reactive powder concrete with steel fibers at elevated temperatures. *Construction and Building Materials,* Volume 41, pp. 844-851.

Zheng, W., Luo, B. & Wang, Y., 2015. Stress-strain relationship of steel-fibre reinforced reactive powder concrete at elevated temperatures. *Materials and Structures,* Volume 48, pp. 2299-2314.

Zheng, W., Wang, R. & Wang, Y., 2014. Experimental study on thermal parameter of reactive powder concrete. *Journal of Building Materials and Structures,* 35(9), pp. 107-114.